Inorganic Chemistry
Article

Inorg. Chem. **2009**, *48*, 7457–7465 **7457**
DOI: 10.1021/ic900037g

Dissolution/Reorganization toward the Destruction/Construction of Porous Cobalt(II)− and Nickel(II)−Carboxylate Coordination Polymers

Miao-Tzu Ding,[†,‡] Jing-Yun Wu,[†] Yen-Hsiang Liu,[§] and Kuang-Lieh Lu*[,†]

[†]*Institute of Chemistry, Academia Sinica, Taipei 115, Taiwan,* [‡]*Department of Chemistry, National Central University, Taoyuan 320, Taiwan, and* [§]*Department of Chemistry, Fu Jen Catholic University, Taipei 242, Taiwan*

Received January 8, 2009

The alkali-metal-cation-induced structural transformation of porous coordination polymers (CPs), $\{A_2[M_3(btec)_2(H_2O)_4]\}_n$ (**1**, A = K, M = Co; **2**, A = K, M = Ni; **3**, A = Cs, M = Co; and **4**, A = Cs, M = Ni; btec = benzene-1,2,4,5-tetracarboxylate), occurred via a unique dissolution/reorganization process in the presence of an alkali chloride (LiCl, NaCl) in water. Treatment of **1** or **2** in an aqueous solution of LiCl resulted in the formation of new metal−carboxylate species $[Co_2(btec)(H_2O)_{10}]\cdot H_2O$ (**5**·H_2O) and $\{Li_2[Ni_3(btec)_2(H_2O)_{10}]\cdot 3.5H_2O\}_n$ (**6**·$3.5H_2O$), respectively. When NaCl was used in place of LiCl under similar reaction conditions, similar dissolution/reorganization processes were observed. The cobalt species **1** and **3** were converted into the metal−carboxylate product $[Na_2Co(btec)(H_2O)_8]_n$ (**7**), whereas the nickel−carboxylate frameworks **2** and **4** were transformed into $\{[Na_4Ni_2(btec)_2(H_2O)_{18}]\cdot 3H_2O\}_n$ (**8**·$3H_2O$). Single-crystal X-ray diffraction analysis revealed that **5**·H_2O is a discrete molecule, which extends to a hydrogen-bonded 3D porous supramolecular network including tetrameric water aggregates. Compound **6**·$3.5H_2O$ adopts a 3D polymeric structure with a novel (2,4,4)-connected net on the basis of a 4-connecting organic node of a btec ligand, a square-planar 4-connecting metallic *trans*-$Ni(O_2C)_4(H_2O)_2$ node, and a 2-connecting octahedral metallic *trans*-$Ni(O_2C)_2(H_2O)_4$ hinge. Compound **7** possesses a 3D polymeric structure comprised of two types of intercrossed (4,4)-layers, a $[Co^{II}(btec)]$-based layer and a $[Na^{I}(btec)]$-based layer, in a nearly perpendicular orientation (ca. 87°). Compound **8**·$3H_2O$ adopted a 2D sheet network by utilizing heterometallic trinuclear clusters of $Na_2Ni(O_2C)_5(H_2O)_9$ as secondary building units. Each sheet is hydrogen-bonded to neighboring units, giving a 3D supramolecular network. It is noteworthy that the dissolution/reorganization process demonstrates the cleavage and reformation of metal−carboxylate bonds, leading to a destruction/construction structural transformation of CPs.

Introduction

Inorganic−organic hybrid materials with dynamic structural transformation properties,[1−3] such as breathing (contraction/expansion or shrinking/extending) transformations[3c,3d,4−11] and conformation-change (crystal-to-amorphous and crystal-to-crystal) transformations,[3a,3b,12−16] are of particular interest

*To whom correspondence should be addressed. Tel.: +886-2-27898518. Fax: +886-2-27831237. E-mail: lu@chem.sinica.edu.tw.

(1) (a) Steed, J. W. *Nature* **2000**, *406*, 943. (b) Halder, G. J.; Kepert, C. J.; Moubaraki, B.; Murray, K. S.; Cashion, J. D. *Science* **2002**, *298*, 1762. (c) Stadler, A.-M.; Kyritsakas, N.; Vaughan, G.; Lehn, J.-M. *Chem.—Eur. J.* **2007**, *13*, 59. (d) Wheaton, C. A.; Jennings, M. C.; Puddephatt, R. J. *J. Am. Chem. Soc.* **2006**, *128*, 15370. (e) Ruben, M.; Payer, D.; Landa, A.; Comisso, A.; Gattinoni, C.; Lin, N.; Collin, J.-P.; Sauvage, J.-P.; de Vita, A.; Kern, K. *J. Am. Chem. Soc.* **2006**, *128*, 15644. (f) Fielden, J.; Long, D.-L.; Cronin, L. *Chem. Commun.* **2004**, 2156. (g) Murugavel, R.; Walawalkar, M. G.; Dan, M.; Roesky, H. W.; Rao, C. N. R. *Acc. Chem. Res.* **2004**, *37*, 763.

(2) (a) Kitagawa, S.; Kitaura, R.; Noro, S.-i. *Angew. Chem., Int. Ed.* **2004**, *43*, 2334 and references therein. (b) Kitagawa, S.; Uemura, K. *Chem. Soc. Rev.* **2005**, *34*, 109 and references therein. (c) Vittal, J. J. *Coord. Chem. Rev.* **2007**, *251*, 1781 and references therein.

(3) (a) Heo, J.; Jeon, Y.-M.; Mirkin, C. A. *J. Am. Chem. Soc.* **2007**, *129*, 7712. (b) Jeon, Y.-M.; Heo, J.; Mirkin, C. A. *J. Am. Chem. Soc.* **2007**, *129*, 7480. (c) Choi, H. J.; Suh, M. P. *J. Am. Chem. Soc.* **2004**, *126*, 15844. (d) Chen, B.; Ma, S.; Hurtado, E. J.; Lobkovsky, E. B.; Liang, C.; Zhu, H.; Dai, S. *Inorg. Chem.* **2007**, *46*, 8705.

(4) (a) Soldatov, D. V.; Ripmeester, J. A.; Shergina, S. I.; Sokolov, I. E.; Zanina, A. S.; Gromilov, S. A.; Dyadin, Y. A. *J. Am. Chem. Soc.* **1999**, *121*, 4179. (b) Soldatov, D. V.; Ripmeester, J. A. *Chem. Mater.* **2000**, *12*, 1827. (c) Manakov, A. Y.; Soldatov, D. V.; Ripmeester, J. A.; Lipkowski, J. *J. Phys. Chem. B* **2000**, *104*, 12111.

(5) (b) Zhang, J.-P.; Lin, Y.-Y.; Zhang, W.-X.; Chen, X.-M. *J. Am. Chem. Soc.* **2005**, *127*, 14162.

(6) (a) Ghosh, S. K.; Bureekaew, S.; Kitagawa, S. *Angew. Chem., Int. Ed.* **2008**, *47*, 3403. (b) Maji, T. K.; Uemura, K.; Chang, H.-C.; Matsuda, R.; Kitagawa, S. *Angew. Chem., Int. Ed.* **2004**, *43*, 3269. (c) Kitaura, R.; Seki, K.; Akiyama, G.; Kitagawa, S. *Angew. Chem., Int. Ed.* **2003**, *42*, 428. (d) Kitaura, R.; Fujimoto, K.; Noro, S.-i.; Kondo, M.; Kitagawa, S. *Angew. Chem., Int. Ed.* **2002**, *41*, 133.

(7) Biradha, K.; Fujita, M. *Angew. Chem., Int. Ed.* **2002**, *41*, 3392.

(8) Carlucci, L.; Ciani, G.; Moret, M.; Proserpio, D. M.; Rizzato, S. *Angew. Chem., Int. Ed.* **2000**, *39*, 1506.

(9) Kepert, C. J.; Hesek, D.; Beer, P. D.; Rosseinsky, M. J. *Angew. Chem., Int. Ed.* **1998**, *37*, 3158.

(10) Chen, C.-L.; Goforth, A. M.; Smith, M. D.; Su, C.-Y.; zur Loye, H.-C. *Angew. Chem., Int. Ed.* **2005**, *44*, 6673.

(11) (a) Halder, G. J.; Kepert, C. J.; Moubaraki, B.; Murray, K. S.; Cashion, J. D. *Science* **2002**, *298*, 1762. (b) Suh, M. P.; Ko, J. W.; Choi, H. J. *J. Am. Chem. Soc.* **2002**, *124*, 10976. (c) Dybtsev, D. N.; Chun, H.; Kim, K. *Angew. Chem., Int. Ed.* **2004**, *43*, 5033. (d) Lu, J. Y.; Babb, A. M. *Chem. Commun.* **2002**, 1340. (e) Deng, H.; Qiu, Y.-C.; Li, Y.-H.; Liu, Z.-H.; Zeng, R.-H.; Zeller, M.; Batten, S. R. *Chem. Commun.* **2008**, 2239.

Published on Web 07/02/2009

in areas of coordination polymers and supramolecules, since they may exist in several distinct extended architectures (or lattices) in response to external stimuli. Such characteristic crystal transformations are frequently triggered by either guest elimination/inclusion[1f,3d,5−12,13a,14c,16] or guest exchange.[3a,3b,13b,14a,14b,15] In addition, a few examples have shown that structural transformation behaviors are driven by physical stimuli, such as light,[17−19] temperature,[1e,3c,12,20−22] acidobasicity,[23] and so forth. It is noteworthy that the transformation of the entire structure of some coordination polymers frequently occurs from one crystalline state to another without destruction of the molecular skeleton or without dissolution and recrystallization of the materials. There are limited examples exhibiting structural transformation through a dissolution/recrystallization process.[24] Rao and co-workers published a series of interesting results where low-dimensional zinc phosphates transformed to complex open-framework structures on heating in water with or without added amines.[25] We recently reported on several charged 3D porous coordination polymers (CPs) with the general formula $\{A_2[M_3(btec)_2(H_2O)_4]\}_n$ (A = K, Cs; M = Co, Ni; btec = benzene-1,2,4,5-tetracarboxylate) that are soluble in an aqueous solution of cesium chloride (CsCl) or potassium chloride (KCl).[26] After dissolution, these compounds reorganize to form new metal−carboxylate species $Cs_2[M(btec)(H_2O)_4]$ (M = Co, Ni) and the stable metal−carboxylate frameworks of $K_2[M_3(btec)_2(H_2O)_4]$ (M = Co, Ni). Note that several products could not be obtained directly using a simple self-assembly synthetic process. Incorporation of alkali metal ions inside the transition metal/carboxylate framework is itself interesting since the alkali ions are relevant as potential adsorption sites in the context of adsorbents for hydrogen.[27] Herein, we report on our ongoing investigations of dissolution/reorganization toward the structural rearrangement of CPs $\{A_2[M_3(btec)_2(H_2O)_4]\}_n$ in aqueous lithium chloride or sodium chloride solutions. Interesting modes of cleavage and reformation of metal−carboxylate donating bonds in coordination frameworks during dissolution/reorganization in aqueous solution were observed, giving rise to extremely rich and diverse structural rearrangements.

Results and Discussion

Dissolution/Reorganization of Cobalt(II)− and Nickel(II)−Carboxylate Frameworks. Porous CPs $\{A_2[M_3(btec)_2(H_2O)_4]\cdot xH_2O\}_n$ (**1**·$6H_2O$, A = K, M = Co, x = 6; **2**·$4H_2O$, A = K, M = Ni, x = 4; **3**·$3H_2O$, A = Cs, M = Co, x = 3; and **4**·$3H_2O$, A = Cs, M = Ni, x = 3) were prepared following procedures reported in the literature.[26] Treatment of **1** or **2** in an aqueous solution of lithium chloride (LiCl) resulted in a dissolution/reorganization process, affording the new metal−carboxylate products $[Co_2(btec)(H_2O)_{10}]\cdot H_2O$ (**5**·H_2O) and $\{Li_2[Ni_3(btec)_2(H_2O)_{10}]\cdot 3.5H_2O\}_n$ (**6**·$3.5H_2O$), respectively. When the lithium chloride was replaced with sodium chloride (NaCl) under similar reaction conditions, dissolution/reorganization processes were also observed. The cobalt species **1** was converted into the metal−carboxylate product $[Na_2Co(btec)(H_2O)_8]_n$ (**7**), whereas the nickel−carboxylate framework **2** was transformed into $\{[Na_4Ni_2(btec)_2(H_2O)_{18}]\cdot 3H_2O\}_n$ (**8**·$3H_2O$). These results are summarized in Scheme 1.

Structural Descriptions of Products Obtained from the Dissolution/Reorganization Process. $[Co_2(btec)(H_2O)_{10}]\cdot H_2O$ (5·H_2O). A structural analysis showed that **5**·H_2O is comprised of two crystallographically distinct

(12) Cheng, X.-N.; Zhang, W.-X.; Chen, X.-M. *J. Am. Chem. Soc.* **2007**, *129*, 15738.
(13) (a) Luo, T.-T.; Hsu, L.-Y.; Su, C.-C.; Ueng, C.-H.; Tsai,; Lu, K.-L. *Inorg. Chem.* **2007**, *46*, 1532. (b) Luo, T.-T.; Liu, Y.-H.; Chan, C.-C.; Huang, S.-M.; Chang, B.-C.; Lu, Y.-L.; Lee, G.-H.; Peng, S.-M.; Wang, J.-C.; Lu, K.-L. *Inorg. Chem.* **2007**, *46*, 10044.
(14) (a) Jung, O.-S.; Kim, Y. J.; Lee, Y.-A.; Park, J. K.; Chae, H. K. *J. Am. Chem. Soc.* **2000**, *122*, 9921. (b) Jung, O.-S.; Kim, Y. J.; Lee, Y.-A.; Chae, H. K.; Jang, H. G.; Hong, J. *Inorg. Chem.* **2001**, *40*, 2105. (c) Jung, O.-S.; Park, S. H.; Kim, K. M.; Jang, H. G. *Inorg. Chem.* **1998**, *37*, 5781.
(15) (a) Min, K. S.; Suh, M. P. *J. Am. Chem. Soc.* **2000**, *122*, 6834. (b) Noro, S.-i.; Kitaura, R.; Kondo, M.; Kitagawa, S.; Ishii, T.; Matsuzaka, H.; Yamashita, M. *J. Am. Chem. Soc.* **2002**, *124*, 2568. (c) Vougo-Zanda, M.; Huang, J.; Anokhina, E.; Wang, X.; Jacobson, A. J. *Inorg. Chem.* **2008**, *47*, 11535.
(16) (a) Barea, E.; Navarro, J. A. R.; Salas, J. M.; Masciocchi, N.; Galli, S.; Sironi, A. *J. Am. Chem. Soc.* **2004**, *126*, 3014. (b) Chen, C.-Y.; Cheng, P.-Y.; Wu, H.-H.; Lee, H. M. *Inorg. Chem.* **2007**, *46*, 5691. (c) Ghosh, S. K.; Zhang, J.-P.; Kitagawa, S. *Angew. Chem., Int. Ed.* **2007**, *46*, 7965. (d) Sun, R.; Li, Y.-Z.; Bai, J.; Pan, Y. *Cryst. Growth Des.* **2007**, *7*, 890. (e) Wang, X.-Y.; Scancella, S. M.; Sevov, C. *Chem. Mater.* **2007**, *19*, 4506.
(17) (a) Nagarathinam, M.; Vittal, J. J. *Chem. Commun.* **2008**, 438. (b) Nagarathinam, M.; Vittal, J. J. *Angew. Chem., Int. Ed.* **2006**, *45*, 4337. (c) Toh, N. L.; Nagarathinam, M.; Vittal, J. J. *Angew. Chem., Int. Ed.* **2005**, *44*, 2237.
(18) (a) Papaefstathiou, G. S.; Zhong, Z.; Geng, L.; MacGillivray, L. R. *J. Am. Chem. Soc.* **2004**, *126*, 9158. (b) Chu, Q.; Swenson, D. C.; MacGillivray, L. R. *Angew. Chem., Int. Ed.* **2005**, *44*, 3569. (c) Papaefstathiou, G. S.; Georgiev, I. G.; Fričić, T.; MacGillivray, L. R. *Chem. Commun.* **2005**, 3974.
(19) (a) Blake, A. J.; Champness, N. R.; Chung, S. S. M.; Li, W.-S.; Schröder, M. *Chem. Commun.* **1997**, 1675. (b) Vela, M. J.; Buchholz, V.; Enkelmann, V.; Snider, B. B.; Foxman, B. M. *Chem. Commun.* **2000**, 2225. (c) Alvaro, M.; Ferrer, B.; Garcķa, H.; Rey, F. *Chem. Commun.* **2002**, 2012. (d) Mal, N. K.; Fujiware, M.; Tanaka, Y. *Nature* **2003**, *421*, 350. (e) Michaelides, A.; Skoulika, S.; Siskos, M. G. *Chem. Commun.* **2004**, 2418. (f) Lee, J. Y.; Hong, S. J.; Kim, C.; Kim, Y. *Dalton Trans.* **2005**, 3716. (g) Briceño, A.; Leal, D.; Atencioa, R.; Delgado, G. D. *Chem. Commun.* **2006**, 3534.
(20) (a) Hu, C.; Englert, U. *Angew. Chem., Int. Ed.* **2006**, *45*, 3457. (b) Hu, C.; Englert, U. *Angew. Chem., Int. Ed.* **2005**, *44*, 2281.
(21) (a) Ranford, J. D.; Vittal, J. J.; Wu, D.; Yang, X. *Angew. Chem., Int. Ed.* **1999**, *38*, 3498. (b) Ranford, J. D.; Vittal, J. J.; Wu, D. *Angew. Chem., Int. Ed.* **1998**, *37*, 1114. (c) Vittal, J. J.; Yang, X. *Cryst. Growth Des.* **2002**, *2*, 259.
(22) (a) Rather, B.; Moulton, B.; Walsh, R. D. B.; Zaworotko, M. J. *Chem. Commun.* **2002**, 694. (b) Legrand, Y.-M.; van der Lee, A.; Masquelez, N.; Rabu, P.; Barboiu, M. *Inorg. Chem.* **2007**, *46*, 9083. (c) Ma, J.-P.; Dong, Y.-B.; Huang, R.-Q.; Smith, M. D.; Su, C.-Y. *Inorg. Chem.* **2005**, *44*, 6143. (d) Shin, D. M.; Lee, I. S.; Cho, D.; Chung, Y. K. *Inorg. Chem.* **2003**, *42*, 7722. (e) Mahmoudi, G.; Morsali, A. *Cryst. Growth Des.* **2008**, *8*, 391. (f) Kepert, C. J.; Rosseinsky, M. J. *Chem. Commun.* **1998**, 31. (g) Chen, B.; Ockwig, N. W.; Fronczek, F. R.; Contreras, D. S.; Yaghi, O. M. *Inorg. Chem.* **2005**, *44*, 181.
(23) (a) Leung, K. C.-F.; Mendes, P. M.; Magonov, S. N.; Northrop, B. H.; Kim, S.; Patel, K.; Flood, A. H.; Tseng, H.-R.; Stoddart, J. F. *J. Am. Chem. Soc.* **2006**, *128*, 10707. (b) Ding, N.; Kanatzidis, M. G. *Angew. Chem., Int. Ed.* **2006**, *45*, 1397.
(24) (a) Friese, V. A.; Kurth, D. G. *Coord. Chem. Rev.* **2008**, *252*, 199. (b) Wu, H. C.; Thanasekaran, P.; Tsai, C. H.; Wu, J. Y.; Huang, S. M.; Wen, Y. S.; Lu, K. L. *Inorg. Chem.* **2006**, *45*, 295. (c) Karabach, Y. Y.; Kirillov, A. M.; da Silva, M. F. C. G.; Kopylovich, M. N.; Pombeiro, A. J. L. *Cryst. Growth Des.* **2006**, *6*, 2200. (d) Zhang, J.-J.; Zhao, Y.; Gamboa, S. A.; Lachgar, A. *Cryst. Growth Des.* **2008**, *8*, 172. (e) Kim, H.-J.; Lee, J.-H.; Lee, M. *Angew. Chem., Int. Ed.* **2005**, *44*, 5810. (f) Lidrissi, C.; Romerosa, A.; Saoud, M.; Serrano-Ruiz, M.; Gonsalvi, L.; Peruzzini, M. *Angew. Chem., Int. Ed.* **2005**, *44*, 2568. (h) Murugavel, R.; Sathiyendiran, M.; Pothiraja, R.; Walawalkar, M. G.; Mallah, T.; Riviére, E. *Inorg. Chem.* **2004**, *43*, 945.
(25) (a) Dan, M.; Rao, C. N. R. *Chem. Commun.* **2003**, 2212. (b) Choudhury, A.; Neeraj, S.; Natarajana, S.; Rao, C. N. R. *J. Mater. Chem.* **2001**, *11*, 1537. (c) Ayi, A. A.; Choudhury, A.; Natarajan, S.; Neeraj, S.; Rao, C. N. R. *J. Mater. Chem.* **2001**, *11*, 1181. (d) Padmanabhan, M.; Joseph, J. C.; Thirumurugan, A.; Rao, C. N. R. *Dalton Trans.* **2008**, 2809.
(26) (a) Wu, J.-Y.; Yang, S.-L.; Luo, T.-T.; Liu, Y.-H.; Cheng, Y.-W.; Chen, Y.-F.; Wen, Y.-S.; Lin, L.-G.; Lu, K.-L. *Chem.—Eur. J.* **2008**, *14*, 7136. (b) Wu, J.-Y.; Ding, M.-T.; Wen, Y.-S.; Liu, Y.-H.; Lu, K.-L. *Chem.—Eur. J.* **2009**, *15*, 3604.
(27) (a) Mulfort, K. L.; Wilson, T. M.; Wasielewski, M. R.; Hupp, J. T. *Langmuir* **2009**, *25*, 503. (b) Mulfort, K. L.; Hupp, J. T. *Inorg. Chem.* **2008**, *47*, 7936. (c) Han, S. S.; Goddard, W. A. III. *J. Am. Chem. Soc.* **2007**, *129*, 8422.

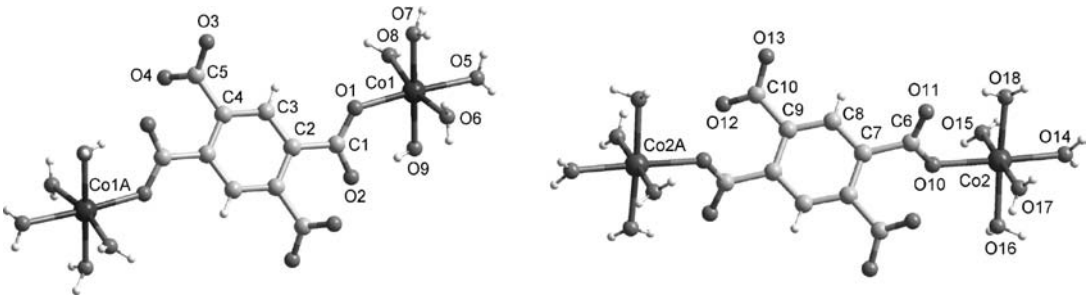

Figure 1. The two crystallographically distinct dinuclear molecules of $[Co_2(btec)(H_2O)_{10}]$ in $\mathbf{5}\cdot H_2O$.

Scheme 1

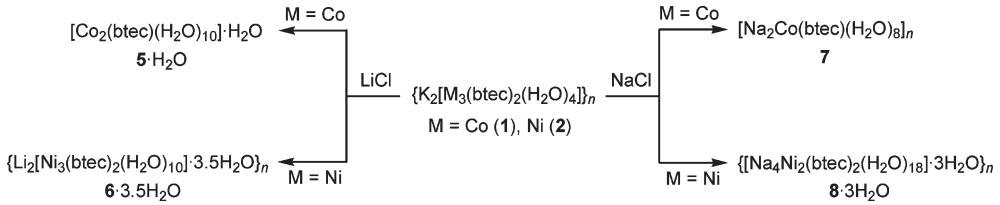

centrosymmetric dinuclear $[Co_2(btec)(H_2O)_{10}]$ molecules, and free water molecules are present in the crystal (Figure 1), which is isostructural and isomorphous with $[Mn_2(btec)(H_2O)_{10}]\cdot H_2O$.[28] Similar molecular structures of $[M_2(btec)(H_2O)_{10}]$ are also observed in $[M_2(btec)(H_2O)_{10}]\cdot 6H_2O$ (M = Co, Ni).[29] For $\mathbf{5}\cdot H_2O$, in which each Co^{II} ion is coordinated by one monodentate carboxylate group of a btec ligand (Co−O = 2.1003(19)−2.101(2) Å) and five water molecules (Co−O = 2.081(2)−2.120(2) Å), each btec ligand is para-bridged to two Co^{II} ions. Crystal packing is stabilized by numerous intermolecular O−H···O hydrogen-bonding interactions (Figure 2a). Interestingly, a hexameric water cluster consisting of a cyclic water tetramer in an *uudd* fashion[30] and two pendent water molecules is formed from two free (O19) and four coordinated (O9 and O16) water molecules. These interactions assist a hydrogen-bonded supramolecular synthon $\{(CoO_6)_4(H_2O)_2\}$, extending to a supramolecular pseudo-(4,4)-layer structure (Figure 2b). The average water···water separation of ca. 2.735 Å within the tetrameric water aggregate is comparable to that for liquid water (2.85 Å)[31] and for other H_2O clusters (2.768−2.834 Å) hosted by metal−organic frameworks.[30b,32]

$\{Li_2[Ni_3(btec)_2(H_2O)_{10}]\cdot 3.5H_2O\}_n$ ($\mathbf{6}\cdot 3.5H_2O$). In $\mathbf{6}\cdot 3.5H_2O$, there are two crystallographically distinct nickel ions: one adopts a distorted *trans*-$Ni(OCO)_4(OH_2)_2$ octahedron with two water molecules (Ni−O = 2.065(7) Å) and four monodentate carboxylate groups (Ni−O = 2.045(5) Å), and the other consists of four water molecules (Ni−O = 2.046(5)−2.057(5) Å) in the basal plane and two monodentate carboxylate groups (Ni−O = 2.075(5) Å) at axial positions, leading to a distorted *trans*-$Ni(OCO)_2(OH_2)_4$ octahedral geometry. Each btec ligand is bridged to four Ni^{II} ions via 1,2,4,5-coordination. The packing diagram reveals that $\mathbf{6}\cdot 3.5H_2O$ exists in a three-dimensional network, which can be described in terms of two building subunits: 2D $[Ni^{II}(btec)]$-based layers and octahedral Ni^{II} hinges. Within the former building subunit, each *trans*-$Ni(OCO)_4(OH_2)_2$ center acts as a square-planar 4-connector, whereas the btec ligands serve as linear linkers, in spite of the fact that the organic multicarboxylate ligand is coordinated to four Ni^{II} ions (i.e., the 4-coordinated organic ligand as a pseudo-2-connecting linear linker), leading to the formation of a (4,4)-net (Figure 3). Interestingly, the [Ni(btec)]-based layer is hinged by the *trans*-$Ni(OCO)_2(OH_2)_4$ centers as linear 2-connecting octahedral hinges, as shown in Figure 4, with the further carboxylate groups of the btec ligand through nickel−carboxylate-directed coordination bonds (2.075(5) Å). This results in the combination of the two building subunits to generate a three-dimensional polymeric structure with a novel (2,4,4)-connected network. The 3D net contains one-dimensional rectangular-shaped channels with an effective window size of approximately 3.8×3.6 Å along the crystallographic *a* axis, which accommodates lithium ions and free water molecules (Figure 5).

$[Na_2Co(btec)(H_2O)_8]_n$ (7). Compound **7** is isostructural and isomorphous with the Ni analogue, $[Na_2Ni(btec)(H_2O)_8]_n$.[33] There is a quarter of a Co^{II} ion, half of a Na^{I} ion, a quarter of a btec ligand, and half of a cobalt-bonded water molecule in the asymmetric unit, as well as one and one-half sodium-bonded water molecules. Each Co^{II} center adopts an octahedral geometry with two water molecules (Co−O = 2.135(2) Å) at the apical positions and four monodentate carboxylate groups (Co−O = 2.1070(16) Å) in the basal plane, while each btec ligand is bridged to four Co^{II} ions via 1,2,4,5-coordination, leading to the formation of a 2D (4,4)-net by regarding both Co^{II} ions and btec ligands to be four-connectors (Figure 6a,b). The overall negative charge of

(28) Rochon, F. D.; Massarweh, G. *Inorg. Chim. Acta* **2001**, *314*, 163.
(29) Rochon, F. D.; Massarweh, G. *Inorg. Chim. Acta* **2000**, *304*, 190.
(30) (a) Ugalde, J. M.; Alkorta, I.; Elguero, J. *Angew. Chem., Int. Ed.* **2000**, *39*, 717. (b) Long, L.-S.; Wu, Y.-R.; Huang, R.-B.; Zheng, L.-S. *Inorg. Chem.* **2004**, *43*, 3798.
(31) Narten, A. H.; Thiessen, W. E.; Blumn, L. *Science* **1982**, *217*, 1033.
(32) (a) Lakshminarayanan, P. S.; Kumar, D. K.; Ghosh, P. *Inorg. Chem.* **2005**, *44*, 7540. (b) Supriya, S.; Das, S. K. *New J. Chem.* **2003**, *27*, 1568.
(33) Sun, L.-P.; Niu, S.-Y.; Jin, J.; Yang, G.-D.; Ye, L. *Eur. J. Inorg. Chem.* **2006**, 5130.

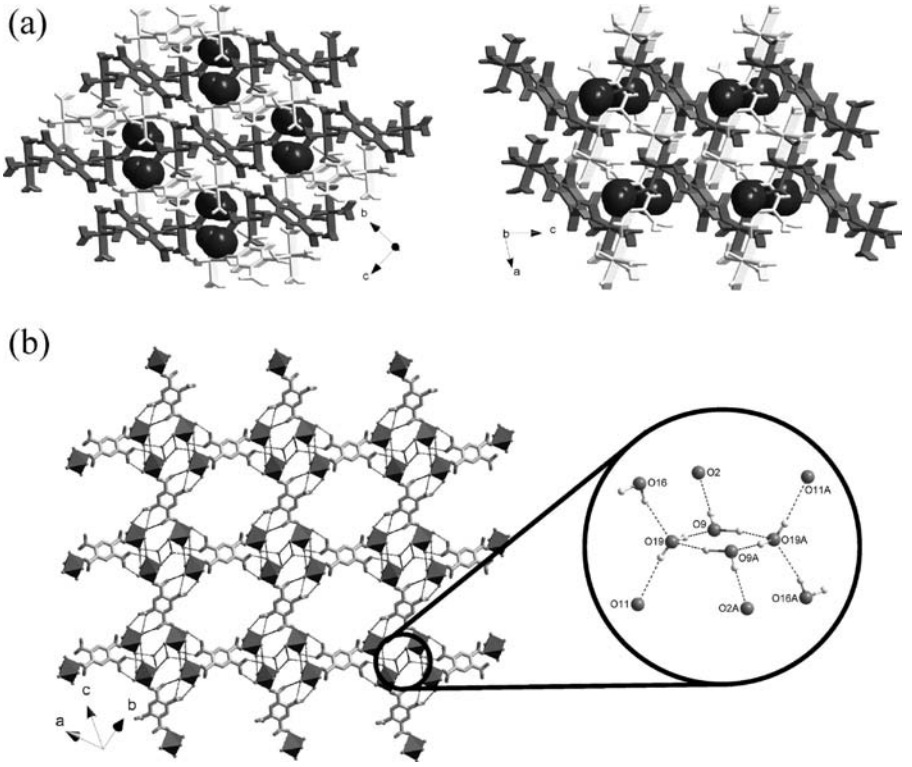

Figure 2. (a) Perspective view of the packing diagrams of $5 \cdot H_2O$. The two crystallographically distinct dinuclear $[Co_2(btec)(H_2O)_{10}]$ molecules, shown in light- and medium-gray colors, and free water molecules are represented as space-filling models. (b) The hydrogen-bonded supramolecular pseudo-(4,4)-layer structure containing cyclic water tetramers in $5 \cdot H_2O$. Its arrangement and immediate environment are highlighted within the circle.

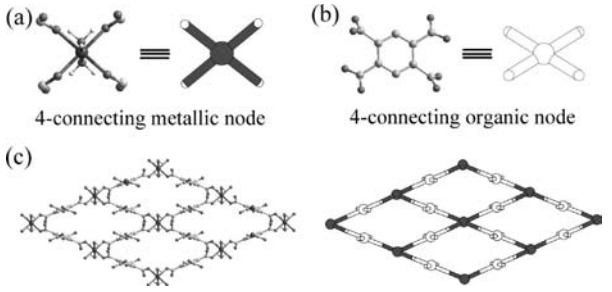

Figure 3. Schematic representations of (a) the metallic and (b) the organic 4-connected nodes in $6 \cdot 3.5H_2O$. (c) Perspective view and schematic representation of the [Ni(btec)]-based 2D layer in a (4,4)-topology, formed by 4-connecting metallic nodes and pseudo-2-connecting organic linkers.

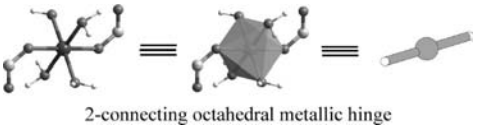

Figure 4. The 2-connecting octahedral metallic hinge of the *trans*-Ni-$(OCO)_2(OH_2)_4$ center in $6 \cdot 3.5H_2O$, shown as ball-and-stick, polyhedron, and schematic representations.

the $[Co^{II}(btec)]$-based layer is balanced by Na^I ions. The octahedrally coordinated Na^I ion is surrounded by three paired monodentate carboxylate groups (Na−O = 2.3379 (19) Å), bridged water molecules (Na−O = 2.5805(12) Å), and terminal water molecules (Na−O = 2.412(2) Å) at trans positions, forming 1D $[(H_2O)_2Na(\mu\text{-}H_2O)]_n$ chains with a Na···Na separation of ca. 4.78 Å. As a result of these sodium−btec contacts, compound **7** possesses a three-dimensional polymeric structure, which can be described in terms of two building subunits: a cationic 1D sodium−hydrate chain of $\{[(H_2O)_2Na^I(\mu\text{-}H_2O)]^+\}_n$ and an anionic 2D (4,4)-layer of a $\{[Co^{II}(btec)]^{2-}\}_n$-net. Nevertheless, it can also be regarded as the result of two types of intercrossed (4,4)-layers, a $[Co^{II}(btec)]$-based layer and a $[Na^I(btec)]$-based layer, in a nearly perpendicular orientation (ca. 87°; Figure 6).

$\{[Na_4Ni_2(btec)_2(H_2O)_{18}]\cdot 3H_2O\}_n$ ($8 \cdot 3H_2O$). In compound $8 \cdot 3H_2O$, the asymmetric unit contains one Ni^{II} ion, two Na^I ions, two halves of the btec ligand, and nine metal-bonded water molecules as well as one and a half free water molecules. Each Ni^{II} center is coordinated by one monodentate carboxylate group (Ni−O = 2.032(3) Å) and five water molecules (Ni−O = 2.016(3)−2.104(3) Å) in an octahedral geometry, of which three water molecules are further bonded to Na^I ions (Na−O = 2.419(3)−2.573(3) Å). Both of the crystallographically distinct Na^I ions show a distorted octahedral NaO_6 core: one being surrounded by one terminal and one bridged water molecule at cis positions (Na−O = 2.336(4)−2.460(3) Å) as well as four monodentate carboxylate groups from two btec ligands (Na−O = 2.303(3)−2.5481(3) Å), and the other surrounded by three terminal and two cis-positioned bridged water molecules (Na−O = 2.332(4)−2.573(3) Å) as well as one monodentate carboxylate group (Na−O = 2.402(3) Å). One of the two crystallographically distinct btec ligands is bridged to two Na^I ions via a bis(ortho-chelating) mode, while the other, in addition to the bis(ortho-chelating) bridged Na^I ions, is para-bridged to two further Na^I ions and two Co^{II} ions (Figure 7). Through three bridged water molecules and one μ,η^1-carboxylate group, one $Ni(O_2C)(H_2O)_5$, one $Na(O_2C)(H_2O)_5$, and one *cis*-$Na(O_2C)_4(H_2O)_2$ core

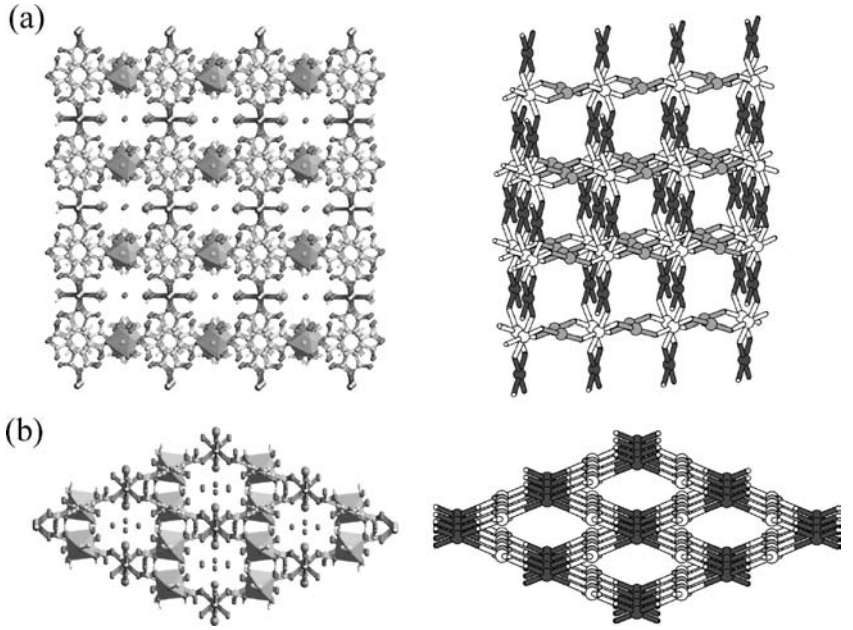

Figure 5. Perspective view and schematic representation of the three-dimensional (2,4,4)-connected network of **6**·3.5H_2O along the crystallographic (a) [100] and (b) [101] directions. Light-gray polyhedron and 2-connector, *trans*-Ni$(OCO)_2(H_2O)_4$; dark-gray 4-connector; *trans*-Ni$(OCO)_4(H_2O)_2$; white 4-connector, btec ligand.

aggregate together to produce a linear heterometallic trinuclear cluster of $Na_2Ni(O_2C)_5(H_2O)_9$ with two Ni···Na separations of 3.5053(19) and 3.5160(18) Å. Such a heterometallic trinuclear cluster is a secondary building unit (SBU) that is linked to three neighboring SBUs via the benzene ring of the btec ligands, forming a two-dimensional sheet network, as shown in Figure 8. Each sheet is hydrogen-bonded (2.58−2.86 Å) to neighboring sheets to produce a three-dimensional supramolecular network.

Examination of the Dissolution/Reorganization Behaviors for $\{Cs_2[M_3(btec)_2(H_2O)_4]\}_n$ (M = Co (3), Ni (4)) in an Aqueous Solution of Sodium Chloride. In addition to the potassium salts of $[M_3(btec)_2(H_2O)_4]^{2-}$ (M = Co, Ni), related investigations involving the cesium salts (**3**·3H_2O and **4**·3H_2O) were also performed in the case of sodium chloride under the same conditions.

When suitable amounts of **3**·3H_2O were added to an aqueous solution of sodium chloride, the red crystals dissolved. Evaporation of the solvent gave reddish block-shaped crystals, along with a large amount of colorless crystals of alkali chloride salts. The red species were identified by a single-crystal X-ray diffraction analysis (INDEX data), indicating that the cell parameters were similar to those of **7**. This result was also confirmed by the powder X-ray diffraction (PXRD) pattern of the reddish-colored samples that had been reassembled from an aqueous solution of **3**·3H_2O and NaCl, which is in good agreement with the simulated and experimental PXRD patterns for **7** (Figure S1, Supporting Information).

On the other hand, when Ni analogue **4**·3H_2O was used to replace the Co derivative **3**·3H_2O in an aqueous solution of sodium chloride, greenish-colored crystals were produced. This product was characterized as **8**·3H_2O on the basis of a comparison of PXRD patterns with patterns simulated from the single-crystal data for **8**·3H_2O (Figure S2, Supporting Information) and an elemental analysis (see the Experimental Section). Furthermore, the single-crystal X-ray diffraction analysis also supports this conclusion.

Discussion. Structural changes in the Co- and Ni-containing CPs, driven by the presence of alkali-metal ions via a dissolution/reorganization process, are observed in the present study.[26b] This phenomenon is significantly different from the solid-state transformations of metal−organic frameworks which show that the structural transformation occurred from one crystalline state to another state without dissolution and recrystallization of the dynamic multifunctional materials. This study initially involved CP **1**−**4** systems and aqueous solutions of KCl or CsCl. The results were the formation of only 3D porous frameworks of $\{K_2[M_3(btec)_2(H_2O)_4]\}_n$ (M = Co (**1**), Ni (**2′**)) and only 1D zigzag chains of $\{Cs_2[M(btec)_2(H_2O)_4]\}_n$ (M = Co (**9**); Ni (**10**)) in the presence of KCl and CsCl, respectively.[26b] Interestingly, a remarkable reversible destruction/construction structural transformation between the 3D porous framework and the 1D zigzag chain structure was demonstrated in the case of Co-containing species. When lithium chloride and sodium chloride are used, instead of potassium chloride and cesium chloride, CPs **1**−**4** undergo dissolution/reorganization case by case, giving rise to extremely rich and diverse structural rearrangements. The metal−carboxylate materials reorganized from aqueous systems of CP **1**/LiCl, CP **2**/LiCl, CP **1** or **3**/NaCl, and CP **2** or **4**/NaCl are structurally characterized as a 0D discrete molecule (**5**·H_2O), a 3D porous framework (**6**·3.5H_2O), a 3D regular network (**7**), and a 2D sheet (**8**·3H_2O), respectively. The reasons for the richness of the structural transformations for CPs **1**−**4** in the presence of LiCl or NaCl in water are unclear but may be related to simple structural changes in CPs **1**−**4** and the KCl or CsCl systems. This could, however, be attributed to the nature of the d-electron configurations of transition metal ions

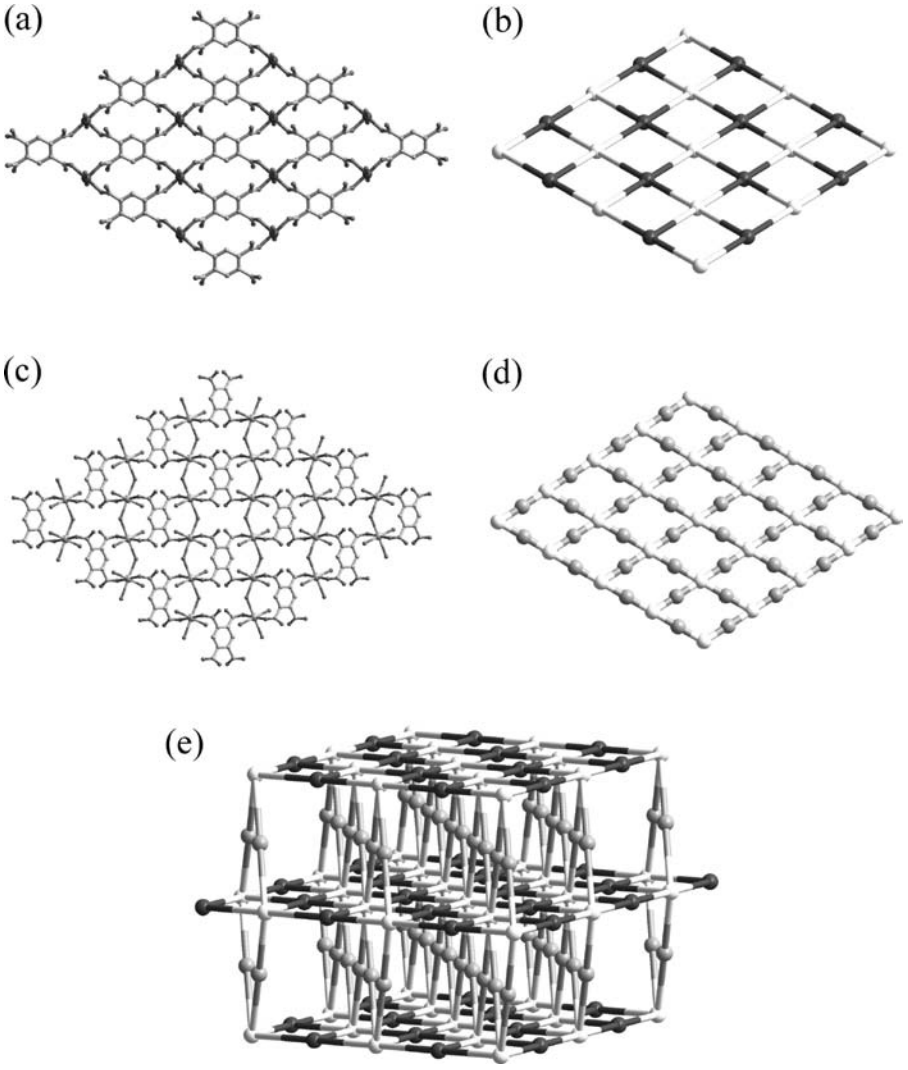

Figure 6. Perspective views of (a) the $[Co^{II}(btec)]$-based (4,4)-layer and (c) the $[Na^{I}(btec)]$-based (4,4)-layer in **7**. Schematic representations are simplified in b and d, respectively. (e) Schematic view of the three-dimensional polymeric architecture of **7**. Dark-gray 4-connector, *trans*-$Co(O_2C-)_4(H_2O)_2$ core; white 4-connector, btec ligand; light-gray 2-connector, $(H_2O)_2Na(\mu\text{-}H_2O)$ core.

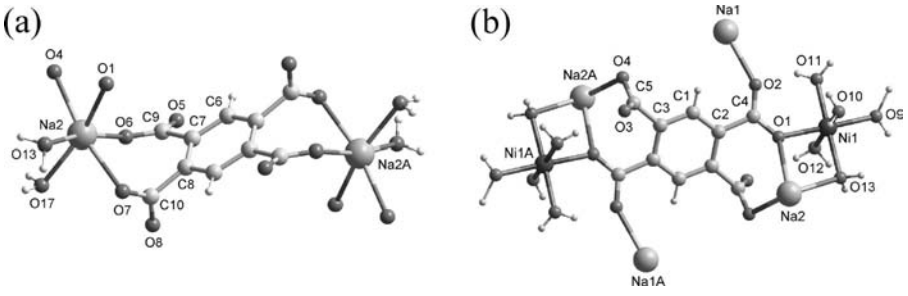

Figure 7. Coordination modes of the two crystallographically distinct btec ligands in $\mathbf{8}\cdot 3H_2O$.

(d^7 for Co^{II} and d^8 for Ni^{II})[34] and the size of the alkali-metal ions (2 Å^3 for Li^I, 3 Å^3 for Na^I, 10 Å^3 for K^I, and 19 Å^3 for Cs^I).[35]

It is noteworthy that the dissolution/reorganization processes leading to the structural conversion of CPs **1**−**4** are the result of the rearrangement of transition metal−carboxylate building blocks. The building blocks in **1**−**4** are trinuclear 8-connectors of $M_3(O_2C)_8(H_2O)_4$, which are coverted to a mononuclear 1-connector ($M(O_2C)(H_2O)_5$) in **5** and **8** as a terminal node, both a linear 2-connector (*trans*-$M(O_2C)_2(H_2O)_4$) and a distorted square-planar 4-connector *trans*-$(M(O_2C)_4(H_2O)_2)$ in **6**, and a distorted square-planar 4-connector (*trans*-$M(O_2C)_4(H_2O)_2$) in **7** as well as a bent 2-connector (*cis*-$M(O_2C)_2(H_2O)_4$) in $\{Cs_2[M(btec)_2(H_2O)_4]\}_n$

(34) (a) Guillou, N.; Livage, C.; Férey, G. *Eur. J. Inorg. Chem.* **2006**, 4963. (b) Livage, C.; Forster, P. M.; Guillou, N; Tafoya, M. M.; Cheetham, A. K.; Férey, G. *Angew. Chem., Int. Ed.* **2007**, *46*, 5877.

(35) Mingos, D. M. P.; Rohl, A. L. *Inorg. Chem.* **1991**, *30*, 3769.

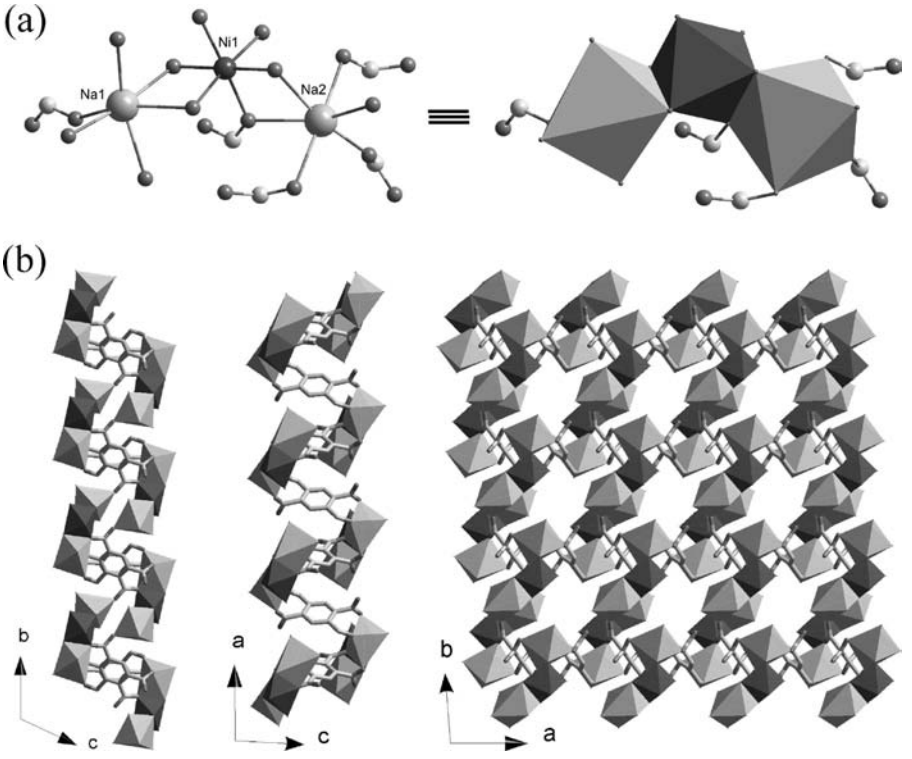

Figure 8. (a) Heterometallic trinuclear SBU of $Na_2Ni(O_2C)_5(H_2O)_9$ in $\mathbf{8}\cdot 3H_2O$, shown as ball-and-stick and edge-sharing polyhedra representations. (b) Views of the two-dimensional sheet network with SBUs linked together via the benzene ring of the btec ligand along the crystallographic *a* (left), *b* (middle), and *c* axes (right). Color scheme: medium gray, O; light gray, C; dark-gray polyhedron, CoO_6 core; light-gray polyhedron, NaO_6 core.

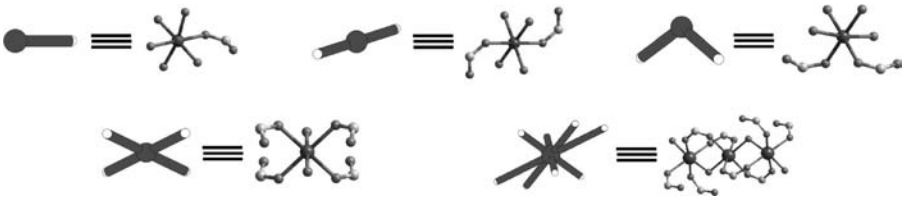

Figure 9. Schematic representations of 1- (terminal, $M(O_2C)(H_2O)_5$), 2- (linear, *trans*-$M(O_2C)_2(H_2O)_4$, and bent, *cis*-$M(O_2C)_2(H_2O)_4$), 4- (distorted square-planar, *trans*-$M(O_2C)_4(H_2O)_2$), and 8-connected (trinuclear cluster, $M_3(O_2C)_8(H_2O)_4$) transition metal−carboxylate building blocks.

(M = Co (**9**), Ni (**10**)) (Figure 9).[26b] As a result, the rearrangement of transition metal−carboxylate building blocks accompanies the metal−carboxylate-donating bond cleavage/formation during dissolution/reorganization. Scheme 2 summarizes the changes in transition metal−carboxylate building blocks in Co− and Ni−carboxylate coordination networks induced by alkali-metal ions (Li^I, Na^I, K^I, and Cs^I) via the dissolution/reorganization process, some of the results are presented from our previous investigations,[26b] which demonstrated the structural transformations in CPs.

Thermal Properties. Thermogravimetric (TG) analysis results for compounds $\mathbf{5}\cdot H_2O$, **7**, and $\mathbf{8}\cdot 3H_2O$ measured under N_2 are shown in Figure S3 (Supporting Information) and are in agreement with microanalytical data. The TG curves reveal that the main weight loss occurs between room temperature and 250 °C, corresponding to the loss of free and coordinated water molecules ($T \leq$ 170 °C for $\mathbf{5}\cdot H_2O$, $T \leq$ 157 °C for **7**, and $T \leq$ 232 °C for $\mathbf{8}\cdot 3H_2O$), before the compounds decompose under N_2 at ca. 430, 370, and 440 °C for $\mathbf{5}\cdot H_2O$, **7**, and $\mathbf{8}\cdot 3H_2O$, respectively. Detailed TG data for the crystalline samples

Scheme 2. Changes in Transition Metal−Carboxylate Building Blocks for the Structural Transformation of CPs **1**−**4** Induced by Alkali−Metal Ions in Aqueous Solutions

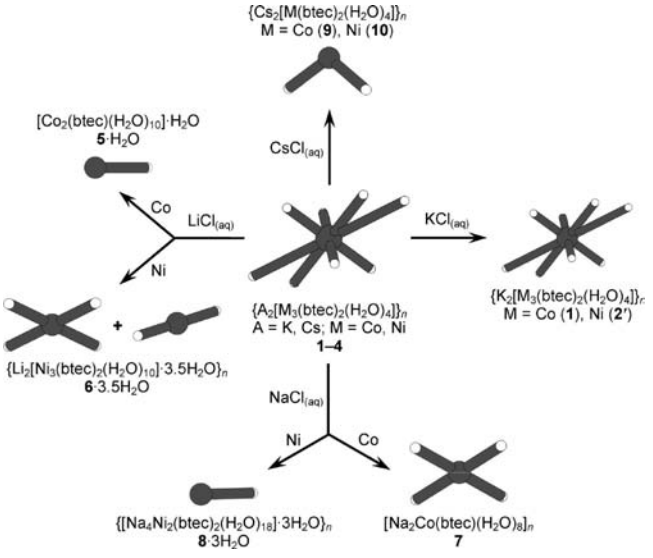

Table 1. Crystallographic Data for $5\cdot H_2O$, $6\cdot 3.5H_2O$, **7**, and $8\cdot 3H_2O$

	$5\cdot H_2O$	$6\cdot 3.5H_2O$	**7**	$8\cdot 3H_2O$
empirical formula	$C_{10}H_{24}Co_2O_{19}$	$C_{20}H_{31}Li_2Ni_3O_{29.5}$	$C_{10}H_{18}CoNa_2O_{16}$	$C_{20}H_{46}Na_4Ni_2O_{37}$
M_w	566.15	933.46	499.15	1087.95
cryst syst	triclinic	monoclinic	monoclinic	triclinic
space group	$P\bar{1}$	$C2/m$	$C2/m$	$P\bar{1}$
a (Å)	9.4058(19)	9.540(2)	15.723(3)	9.6710(7)
b (Å)	10.215(2)	19.812(5)	9.5571(19)	10.2810(7)
c (Å)	11.096(2)	11.151(3)	6.1123(12)	11.1449(7)
α (deg)	87.82(3)	90	90	114.761(4)
β (deg)	77.29(3)	113.684(10)	92.83(3)	92.333(4)
γ (deg)	70.21(3)	90	90	93.158(4)
V (Å^3)	977.8(3)	1930.2(8)	917.4(3)	1002.22(12)
Z	2	2	2	1
T (K)	293(2)	293(2)	293(2)	293(2)
λ (Å)	0.71073	0.71073	0.71073	0.71073
D_{calcd} (g cm^{-3})	1.923	1.606	1.807	1.803
μ (mm^{-1})	1.793	1.546	1.066	1.104
F_{000}	580	954	510	562
GOF	1.052	0.959	1.123	0.777
$R_1{}^a$ ($I > 2\sigma(I)$)	0.0295	0.0629	0.0294	0.0516
$wR_2{}^b$ ($I > 2\sigma(I)$)	0.0779	0.1784	0.0753	0.0890
$R_1{}^a$ (all data)	0.0450	0.1117	0.0329	0.1469
$wR_2{}^b$ (all data)	0.0847	0.1887	0.0775	0.1030
$\Delta\rho_{max}/\Delta\rho_{min}$ (e Å^{-3})	0.431/−0.499	1.049/−0.542	0.243/−0.431	0.415/−0.528

$^a R_1 = \sum ||F_o - F_c||/\sum |F_o|$. $^b wR_2 = \{\sum [w(F_o^2 - F_c^2)^2]/\sum [w(F_o^2)^2]\}$.

of $5\cdot H_2O$, **7**, and $8\cdot 3H_2O$ are summarized in Table S1 (Supporting Information).

Conclusions

In this study, dissolution/reorganization toward the structural transformation of CPs $\{A_2[M_3(btec)_2(H_2O)_4]\}_n$ (A = K, Cs; M = Co, Ni), accompanied by the rearrangement of transition metal−carboxylate building blocks via bond cleavage/formation, occurred in the presence of alkali-metal chloride (LiCl and NaCl) in water, leading to the formation of new metal−carboxylate species. Taking a simple survey, dissolution/reorganization processes reveal the results, case by case in the work presented here (LiCl or NaCl); therefore, CPs **1**−**4** would give rise to extremely rich and diverse structural rearrangements. The resulting metal−carboxylate materials are a 0D discrete molecule ($5\cdot H_2O$), a 3D porous (2,4,4)-connected framework ($6\cdot 3.5H_2O$), a 3D regular network (**7**), and a 2D sheet ($8\cdot 3H_2O$). In comparison, the results regarding aqueous systems of CPs **1**−**4** and KCl or CsCl are relatively simple and afforded only a 3D porous framework of $\{K_2[M_3(btec)_2(H_2O)_4]\}_n$ and only a 1D zigzag chain of $\{Cs_2[M(btec)_2(H_2O)_4]\}_n$, respectively. This may be attributed to the nature of the d-electron configurations of transition metal ions (Co^{II} and Ni^{II}) and the size of the alkali-metal ions (Li^I, Na^I, K^I, and Cs^I) used.

Experimental Section

Materials and Instruments. Chemical reagents were purchased commercially and were used as received without further purification. Solvated CPs $\{A_2[M_3(btec)_2(H_2O)_4]\cdot xH_2O\}_n$ ($1\cdot 6H_2O$, A = K, M = Co, x = 6; $2\cdot 4H_2O$, A = K, M = Ni, x = 4; $3\cdot 3H_2O$, A = Cs, M = Co, x = 3; and $4\cdot 3H_2O$, A = Cs, M = Ni, x = 3) were prepared following literature procedures.[26] TG analyses were performed under nitrogen with a Perkin-Elmer TGA-7 TG analyzer. PXRD measurements were recorded on a Siemens D-5000 diffractometer at 40 kV, 30 mA for Cu Kα (λ = 1.5406 Å), with a step size of 0.02° in θ and a scan speed of 1 s per step size. Elemental analyses were carried out on a Perkin-Elmer 2400 CHN elemental analyzer.

Dissolution/Reorganization of Porous CPs 1 and 2 in Aqueous Solutions of Lithium Chloride. Entry 1: $[Co_2(btec)(H_2O)_{10}]\cdot H_2O$ ($5\cdot H_2O$). CP $1\cdot 6H_2O$ (28.0 mg, 3.0×10^{-2} mmol) was dissolved in an aqueous solution of lithium chloride (1.0 M, 5 mL, 5 mmol). Pink crystals of $5\cdot H_2O$ (9.0 mg, 1.6×10^{-2} mmol, 35% based on Co^{2+}) appeared after the solution was allowed to stand for ca. 60 days. Anal. found: C, 21.02; H, 4.15%. Calcd for $C_{10}H_{24}Co_2O_{19}$: C, 21.22; H, 4.27%.

Entry 2: $\{Li_2[Ni_3(btec)_2(H_2O)_{10}]\cdot 3.5H_2O\}_n$ ($6\cdot 3.5H_2O$). CP $2\cdot 4H_2O$ (34.6 mg, 3.9×10^{-2} mmol) was dissolved in an aqueous solution of lithium chloride (1.0 M, 5 mL, 5 mmol). Green crystals of $6\cdot 3.5H_2O$ appeared after the solution was allowed to stand for ca. 90 days.

Dissolution/Reorganization of Porous CPs 1−4 in Aqueous Solutions of Sodium Chloride. Entry 1: $[Na_2Co(btec)(H_2O)_8]_n$ (7). CP $1\cdot 6H_2O$ (31.3 mg, 3.3×10^{-2} mmol) was dissolved in an aqueous solution of sodium chloride (1.0 M, 5 mL, 5 mmol). Red crystals of **7** (18.7 mg, 3.7×10^{-2} mmol, 56% based on $btec^{4-}$) appeared after the solution was allowed to stand for ca. 60 days. Anal. found: C, 24.05; H, 3.50%. Calcd for $C_{10}H_{18}CoNa_2O_{16}$: C, 24.06; H, 3.63%.

Entry 2: $\{[Na_4Ni_2(btec)_2(H_2O)_{18}]\cdot 3H_2O\}_n$ ($8\cdot 3H_2O$). CP $2\cdot 4H_2O$ (72.5 mg, 8.1×10^{-2} mmol) was dissolved in an aqueous solution of sodium chloride (1.0 M, 5 mL, 5 mmol). Green crystals of $8\cdot 3H_2O$ (20.7 mg, 1.9×10^{-2} mmol, 24% based on $btec^{4-}$) appeared after the solution was allowed to stand for ca. 30 days. Anal. found: C, 22.47; H, 3.91%. Calcd for $C_{20}H_{46}Na_4Ni_2O_{37}$: C, 22.08; H, 4.26%.

Entry 3. CP $3\cdot 3H_2O$ (36.6 mg, 3.4×10^{-2} mmol) was dissolved in an aqueous solution of sodium chloride (1.0 M, 7 mL, 7 mmol). After the solution was allowed to stand for ca. 40 days, red crystals of **7**, identified by PXRD analysis and a comparison of cell parameters (INDEX data) from a single-crystal X-ray diffraction analysis, were obtained. Yield: 65% based on $btec^{4-}$ (22.3 mg, 4.5×10^{-1} mmol). Anal. Found: C, 23.96; H, 3.60. Calcd for $C_{10}H_{18}CoNa_2O_{16}$ (**7**): C, 24.06; H, 3.63.

Entry 4. CP $4\cdot 3H_2O$ (31.2 mg, 2.9×10^{-2} mmol) was dissolved in an aqueous solution of sodium chloride (1.0 M, 12 mL, 12 mmol). After the solution was allowed to stand for ca. 80 days, green crystals of $8\cdot 3H_2O$, identified by PXRD analysis and a comparison of cell parameters (INDEX data) from a single-crystal X-ray diffraction analysis, were obtained. Yield: 82%

based on $btec^{4-}$ (25.9 mg, 2.4×10^{-1} mmol). Anal. Found: C, 22.31; H, 3.90. Calcd for $C_{20}H_{46}Na_4Ni_2O_{37}$ ($\mathbf{8}\cdot 3H_2O$): C, 22.08; H, 4.26.

Crystallographic Determination. Single-crystal X-ray diffraction analysis was performed by using an Enraf Nonius CAD4 diffractometer for $\mathbf{5}\cdot H_2O$ and **7** and a Bruker P4 diffractometer for $\mathbf{6}\cdot 3.5H_2O$ and $\mathbf{8}\cdot 3H_2O$ equipped with graphite monochromatized Mo Kα radiation ($\lambda = 0.71073$ Å). The structures were solved by direct methods and refined by the full-matrix least-squares method on F^2 values using the WINGX[36] and SHELX-97[37] program packages. Anisotropic thermal factors were assigned to non-hydrogen atoms, except the oxygen atoms of the free water molecules in $\mathbf{6}\cdot 3.5H_2O$. Hydrogen atoms were placed in calculated positions with isotropic displacement parameters. The aqua hydrogen atoms in $\mathbf{5}\cdot H_2O$, **7**, and $\mathbf{8}\cdot 3H_2O$ as well as those of coordinated water molecules in $\mathbf{6}\cdot 3.5H_2O$ were located from difference Fourier maps and refined isotropically. No attempt was made to locate the hydrogen atoms of the free water molecules in $\mathbf{6}\cdot 3.5H_2O$. Lithium metal ions were assigned for the charge compensation in $\mathbf{6}\cdot 3.5H_2O$. The defined Li ion is located at a special position with a site of occupancy of 0.5, which fully meets the requirements for charge compensation. In addition, the thermal factor of the defined Li ion is more reasonable than that of a water oxygen atom. The disorder of lithium ions is possible considering the high anisotropy of thermal motion. Experimental details for X-ray data collection and the refinements are summarized in Table 1.

(36) Farrugia, L. J. *J. Appl. Crystallogr.* **1999**, *32*, 837.
(37) Sheldrick, G. M. *SHELX−97* (including SHELXS and SHELXL); University of Gottingen: Gottingen, Germany, 1997.

Acknowledgment. We thank Academia Sinica and the National Science Council of Taiwan for financial support.

Supporting Information Available: Full crystallographic details (CIF) for $\mathbf{5}\cdot H_2O$, $\mathbf{6}\cdot 3.5H_2O$, **7**, and $\mathbf{8}\cdot 3H_2O$ are provided. Powder X-ray diffractions patterns, TG diagrams, and data analyses for $\mathbf{5}\cdot H_2O$, **7**, and $\mathbf{8}\cdot 3H_2O$. This material is available free of charge via the Internet at http://pubs.acs.org.